JOURNAL OF MATERIALS SCIENCE 24 (1989) 2917–2922

Fracture behaviour of uPVC thin tubes at high loading rates

Part 2 *Validity of fracture toughness tests and the effects of rate*

M. B. JAMARANI
Mechanical Engineering Department, Imperial College, Exhibition Road, London SW7, UK
P. E. REED, W. R. DAVIES*
*Department of Materials, and *Department of Mechanical Engineering, Queen Mary College, Mile End Road, London E1 4NS, UK*

Impact tests and fracture toughness tests were carried out using thin cylindrical specimens of unplasticized poly(vinyl chloride). The specimens, both pre-notched and unnotched, were internally pressurized to fracture at high loading rates, using a conventional shock tube. Over the wide range of the applied loading rates, failure of the pre-notched specimens occurred in a completely brittle mode, while in the case of unnotched specimens, a transition from "semi-brittle" to brittle fracture occurred over the same range of loading rate. Adopting standard linear elastic fracture mechanics (LEFM) analysis, a validity criterion is suggested based on the variation of the extent of crack tip plasticity with the loading rate, as calculated by Dugdale and Irwin models. It is suggested that the decrease in the plastic zone size with increasing rate, affects the size requirement for a valid (plane strain) fracture toughness value.

1. Introduction

In a previous paper [1], fracture mechanics concepts were utilized to describe the failure behaviour of thin unplasticized poly(vinyl chloride) (uPVC) tubes at high loading rates. It was shown that the considerations of rate effects in determining fracture parameters of polymers at impact are of paramount importance. The investigation reported here provides a critical examination of the concepts of crack tip plasticity and size effects.

Consideration of Folias' bending correction factor for thin cylindrical specimens, results in a fracture criterion of the form

$$\sigma_f = K_c \Big/ \left[\pi a \left(1 + 1.54 \frac{a^2}{Rh} \right) \right]^{1/2} \quad (1)$$

where a is the half-crack length, R the radius, h the thickness of the cylindrical specimens, σ_f is the fracture stress, and K_c is the stress intensity factor [1].

Because structural materials deform plastically above their yield stress, it is well known that due to the stress singularity at the crack tip, in reality even the most brittle failures involve some plastic deformation near the tip of the crack. Furthermore, the validity of the measured fracture toughness values (as the material property) depends on the extent of this plastic zone. Usually, if the length of the zone constitutes less than a tenth of the material thickness, the state of stress is considered to be "plain strain" and K_c, is known to be constant representing a material property.

Theoretical consideration of the extent of the plastic zone shows that it depends on the intensity of the stress field at the crack tip, K, as well as the yield stress of the material, σ_y. As both K and σ_y are rate-dependent parameters, the plastic zone size varies with the loading rate, leading to the conclusion that for a constant thickness material, the state of stress changes as the loading rate is varied.

2. Experimental procedure

Thin cylindrical specimens 50.8 mm long, 0.381 mm thick and 38.1 mm in diameter, were broken in a conventional shock tube by rapid internal pressurization. The specimen formed an integral part of the shock tube, and was mounted such that it was essentially a freely supported body (see Fig. 1). Details of the technique used have been described previously [2, 3]. Nominally infinite loading rates (step loading) as well as ramp loading at high rates, were obtained using the same apparatus. Sharp longitudinal cracks of varying lengths were introduced in some specimens, while others were left uncracked. Both the apparatus and the specimens were instrumented such that the pressure pulse and the resulting strain in the specimen, were accurately monitored throughout the tests to the point of fracture. The strain system acting in the flawed cylinders is considered to be predominantly a unidirectional hoop stress given by

$$\sigma_\theta = PR/h \quad (2)$$

where P is the internal pressure, R the radius of the

0022–2461/89 $03.00 + .12

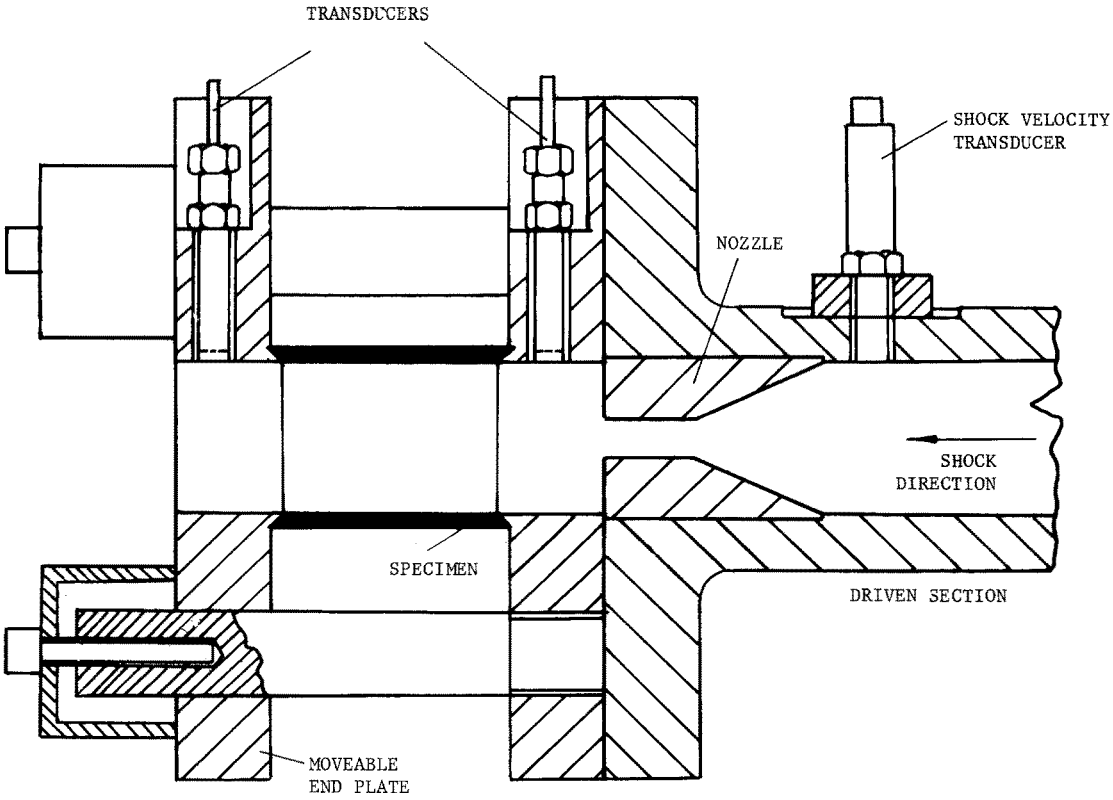

Figure 1 Schematic diagram of the specimen support assembly on the shock tube.

specimen, and h its thickness. The main advantages of the shock tube technique are the facility to provide a wide range of rapid loading rates, using the same apparatus and specimen geometry, minimum interaction between the specimen and apparatus, as well as the essentially uniform stress field set up throughout the entire length of the specimen.

3. Results and discussion

3.1. Crack tip plastic zone

In order to utilize the fracture mechanics concepts of Griffith [4] and Irwin [5] to predict the failure stress–critical crack length relationship in thin cylindrical tubes, Equation 1 can be modified to account for the effects of relaxation due to plastic deformation at the crack tip. Considerations of the crack tip plasticity leads to the conclusion that the occurrence of the plastic deformation makes the crack behave as if it were longer than its physical size and hence the concept of equivalent elastic crack is introduced. Under such conditions, the displacements tend to be longer and the stiffness lower than a purely elastic case. It has been shown by Irwin that the crack may be viewed as having a notional tip at a distance, r_y, ahead of the real tip, where r_y is the radius of the plane stress plastic zone region at the tip of the crack. According to Irwin, r_y is given by

$$r_y = \frac{K^2}{2\pi\sigma_y^2} \tag{3}$$

Therefore, at the onset of crack growth instability, the extent of plastic zone may be given by

$$r_{yc} = \frac{K_c^2}{2\pi\sigma_y^2} \tag{4}$$

As both K_c and σ_y are rate-dependent parameters, the plastic zone size also varies with the loading rate. The dependence of K_c on loading rate, $\dot{P}$, has been discussed previously [1], where it was shown that for $\dot{P} > 250\,\text{MPa sec}^{-1}$ the fracture toughness decreased linearly with the loading rate. The relationship between K_c and $\dot{P}$ is given by

$$K_c = (-6.44 \times 10^{-4})\dot{P} + 1.70 \tag{5}$$

where $\dot{P}$ is in MPa sec^{-1} and K_c in $\text{MPa m}^{1/2}$.

The yield behaviour of polymers is also dependent upon the rate of the test. Generally, the yield stress is found to increase as strain rate ($\dot{\varepsilon}$) is increased. This effect combined with the effect of temperature on yield stress has been investigated by many workers using the Eyring theory of viscosity [6]. According to this theory, a plot of σ_y against $\log \dot{\varepsilon}$ gives a straight line at any given temperature. This has been experimentally verified by Bauwens-Crowet *et al.* [7] for many polymers including PVC, over wide ranges of temperature and strain rate. The range of rates used in the present investigation, although wide in terms of the loading rate, is relatively limited with respect to strain rates [3]. The range of loading rates used varied from $100\,\text{MPa sec}^{-1}$ to nominally infinite (i.e. step loading), which led to strain rates in the range of 2 to $100\,\text{sec}^{-1}$, respectively. Therefore, a linear relationship between σ_y and $\dot{P}$ may be assumed without expecting large discrepancies. From the Bauwens-Crowet results on PVC at room temperature, this relationship may be found to be

$$\sigma_y = 0{\cdot}044\dot{P} + 42{\cdot}5 \tag{6}$$

where $\dot{P}$ is in MPa sec^{-1} and σ_y in MPa. The extent of the plastic zone at instability may therefore be found for various loading rates using Equations 3 to 6. This is shown in Fig. 2 as a plot of r_y against $\dot{P}$.

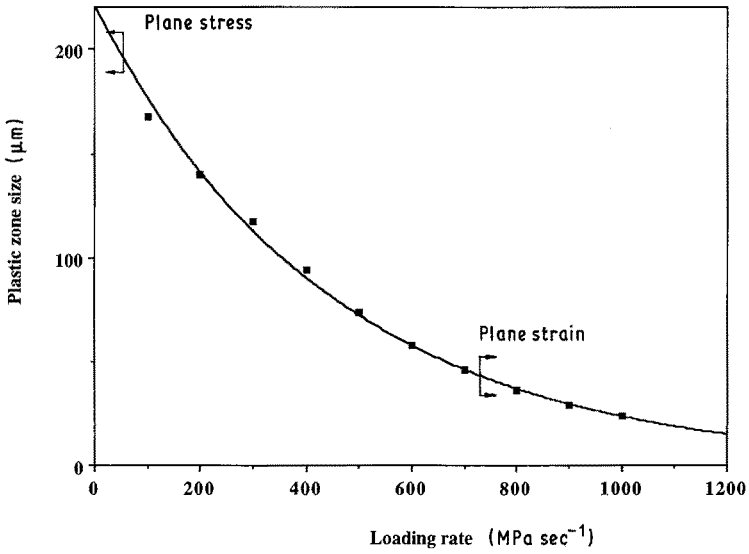

Figure 2 Variation of the plastic zone size with loading rate (by Irwin model).

The above analysis is based on the assumption that the plastic zone is of circular shape. Another relationship between the applied stress, crack length and the extent of plasticity for plane stress may be derived by using Westergaard's stress function [8]. The model followed by Dugdale, also considers an effective crack which is longer than the physical crack. In this case, by considering the stresses within the plastic zone which tend to close the crack, and the elastic strain distribution immediately ahead of the plastic zone, the following relationship for the plastic zone can be obtained

$$r_y = \frac{\pi}{8}\frac{K^2}{\sigma_y^2} \tag{7}$$

It can be seen that the Dugdale's estimate of plastic zone size is somewhat larger than that suggested by Irwin. Substituting again for K_c and σ_y in terms of the loading rate, $\dot{P}$, variations of the extent of plasticity may be found with the loading rate. This is shown in Fig. 3.

3.2. Fracture toughness validity

It is well known that the state of stress in the crack tip region (plane stress or plane strain) will affect the plastic zone size and shape. The size of the plastic zone varies through the thickness of the specimen. At the specimen surfaces the normal stresses are zero and therefore a state of plane stress exists, while the centre tends towards plane strain, provided the specimen is sufficiently thick. The depth of the plane stress region is known to be of the same order as the extent of the plane stress plastic zone (i.e. Equation 3); however, the thickness must be somewhat larger than $2r_y$ to achieve plane strain in the centre. There are some empirical rules for estimating whether the condition is predominantly plane stress or plane strain. Full plane stress may be expected if the calculated size of the plane stress plastic zone is of the order of half the specimen thickness. A predominantly plane strain situation may be expected when the calculated size of the plane stress plastic zone, which exists at the plate surface, is less than a tenth of the specimen thickness.

This latter condition may also be used as a criterion for a valid fracture toughness value because it defines the minimum thickness required for a plane strain situation in terms of the plastic zone size, r_y. The thickness requirement for the plane strain behaviour is

$$h \geqslant 10r_y \tag{8}$$

This has been found in a more accurate way to be [9]

$$h \geqslant 2.5\frac{K_c^2}{\sigma_y^2} \tag{9}$$

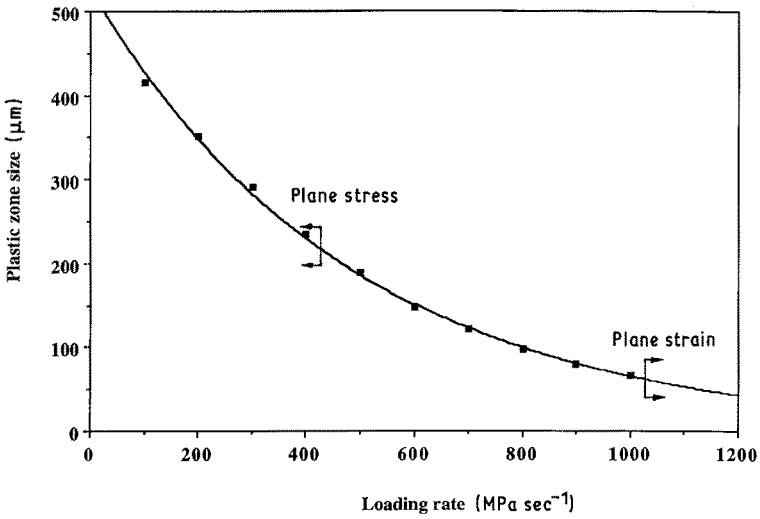

Figure 3 Variation of the plastic zone size with loading rate (by Dugdale model).

or using Equation 4

$$h \geqslant 7.85 r_y \qquad (10)$$

in order to examine the significance of this in terms of the loading rate, Equations 5 and 6 may be substituted into Equation 9 and the range of $\dot{P}$ for a valid fracture toughness value be found. Alternatively, because in this case the thickness of the specimens is held constant, (i.e. 0.381 mm), using the graphs in Figs 2 and 3 and substituting for the thickness in Equation 10, it is possible to find the range of the loading rates for a valid plane strain fracture toughness value. These are shown in Figs 2 and 3. It can be seen that, for example, in the case of Irwin's model, a predominantly plane strain situation exists only when the loading rate is higher than about 700 MPa sec^{-1}. This would mean that, only for loading rates above 700 MPa sec^{-1} the plastic zone size is small enough for the plane strain criterion to be satisfied. Only in such cases could the obtained values of the stress intensity factor, K_c, be taken as a material property (i.e. fracture toughness) at that particular loading rate. This limit is also shown for the plastic zone size found from Dugdale's model (Fig. 3).

Application of the plane stress criterion (i.e. plastic zone size of the same order as $h/2$) leads to the second limit shown in Figs 2 and 3. According to the Irwin model, predominantly plane stress conditions should exist at all loading rates less than about 50 MPa sec^{-1}. For loading rates between the two limiting values, (i.e. $50 \leqslant \dot{P} \leqslant 700$ in the Irwin model) a mixed stress state exists. A model sometimes used is to consider two values of fracture toughness, K_{c1} and K_{c2}, in plane stress and plane strain, respectively [10].

3.3. Transition in the fracture mode

Fig. 4 shows the variation of the fracture stress with loading rate for both notched and unnotched specimens. It can be seen that for the notched specimens σ_f decreases with increasing loading rate when this is greater than 200 MPa sec^{-1} ($1/\dot{P} < 50 \times 10^{-4}$ (MPa $sec^{-1})^{-1}$). However, in the case of unnotched specimens, the fracture stress increases with the loading rate over the same range of rates. Fig. 4 also shows the variation in yield stress, σ_y, with the equivalent inverse loading rate over the same range of rates as reported by Bauwens-Crowet *et al.* [7] for PVC. The use of the inverse loading rate overcomes the difficulty of expressing the case of step loading (i.e. nominally infinite loading rate). It can be seen that all the pre-notched and unnotched specimens fail at stresses below the yield stress of the material further indicating a brittle fracture at all loading rates. On the other hand, in the case of unnotched specimens where fracture initiates from inherent flaws pre-existing in the material, a transition in the mode of failure seems to occur in the region of $\dot{P} = 700$ MPa sec^{-1}, such that:

(a) for $\dot{P}$ less than 700 MPa sec^{-1} yield stress is reached before the fracture stress, and therefore the failure mechanism is not brittle;

(b) for $\dot{P}$ more than about 700 MPa sec^{-1} fracture stress falls below the yield stress, indicating a brittle failure.

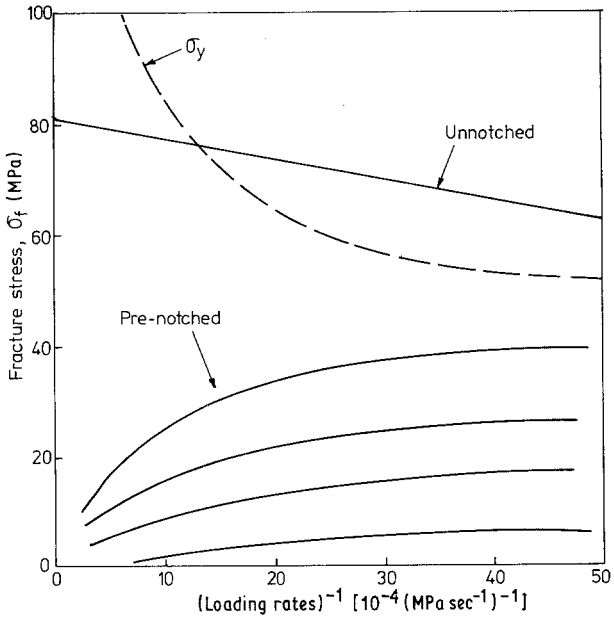

Figure 4 Fracture stress variation with inverse loading rates for notched and unnotched specimens.

It may also be noted that, this transition region corresponds to the loading rates at which a predominantly plane strain situation prevailed. Therefore, while decreasing the loading rate results in a change of stress state within the specimens from plane strain to plane stress, this does not lead to a brittle–ductile transition in the fracture of pre-notched specimens. On the other hand, it may be suggested that in the case of unnotched specimens a transition to a *semi-brittle* mode of fracture begins to occur at a loading rate corresponding to the region where a mixed stress state system exists.

3.3. Failure of unnotched specimens

Because one objective of fracture mechanics is to provide means of predicting failure initiated from natural flaws, it is necessary to examine the applicability of the fracture toughness data (obtained from tests on artificially notched specimens) to the impact failure of thin tubes initiated from inherent flaws (i.e. unnotched specimens).

It has been found that in polymers when the flaw size is reduced below a critical level, the usual fracture mechanics criterion relating the strength to the flaw size (i.e. $\sigma_f = K_c/Ya^{1/2}$) no longer operates. In such cases, polymers behave as if they contain natural flaws of the same size, termed inherent or intrinsic flaws. It is known that these flaws are not usually present in the material before deformation but appear to be formed during loading and they are related to crazes which nucleate under stress and break down to form cracks [11]. Considering the K_c variations with the loading rate, the relationship between fracture stress and crack size for two values of loading rates are shown schematically in Fig. 5. The meaning of this simple graphical presentation is that so long as the combination of stress and flaw size at any loading rate is below the line corresponding to that rate, the critical condition would not be expected. However, if the combination is on or above the line, the consequence of sudden, unstable growth must be considered. Furthermore, it

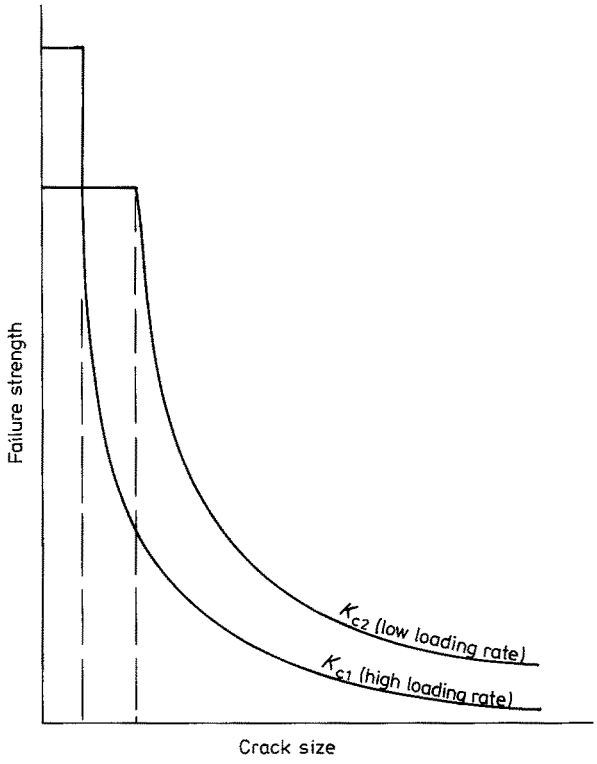

Figure 5 Relationship between the failure stress and the critical crack length for two values of the stress intensity factor.

is noted that there is a yield stress cut-off on these graphs at small values of crack lengths meaning that in those regions, the yield stress, σ_y, is reached before the fracture stress, σ_f, so that failure is controlled by a yield mechanism and the linear elastic fracture mechanics (LEFM) does not operate. Because σ_y is also rate dependent and its value increases with increasing rate, it can be seen that for lower K_c values, smaller minimum flaw lengths are needed for valid LEFM. This is clearly shown in Fig. 5 where the curve corresponding to a lower loading rate is cut off at a longer crack length. Comparison of the two curves in Fig. 5 shows that, although fracture stress is found to be greater at lower rates of loading, because of the material's greater tendency to yield at lower rates, deviation from theoretical curves occurs at larger crack lengths and the observed fracture stress of normal (uncracked) samples is found to be higher at higher rates. Therefore, in order to have valid LEFM, it may be suggested that the fracture toughness values obtained by testing on pre-notched specimens may be applied to predict fracture strength of unnotched tubes providing that the loading rates are in excess of a minimum value.

The relationship between the crack length, stress intensity factor and fracture stress, for brittle fracture of a thin-walled cylindrical tube is given in Equation 1. This equation includes the Folias factor correction for the bending moments in the vicinity of the longitudinal crack under the action of internal pressure. The value of K_c will depend on the loading rate applied. By substituting the yield stress, σ_y, as the fracture stress in Equation 1, using the K_c value appropriate to the loading rate, a value for the minimum crack length (a_m), necessary for brittle failure at each loading rate may be obtained. Equation 1 then becomes

$$\sigma_y = \frac{K_c}{\left[\pi a_m \left(1 + 1.54 \frac{a_m^2}{Rh}\right)\right]^{1/2}} \quad (11)$$

where K_c and σ_y correspond to a specific loading rate. The variation in a_m with loading rate is shown in Fig. 6 over the range of loading rates used in this work for unnotched specimens. This graph shows that because at high loading rates K_c is small and σ_y is large, the value of a_m becomes very small and almost any intrinsic flaw can cause brittle failure.

Alternatively, fracture stresses found from tests on unnotched specimens together with K_c values at the corresponding loading rate may be substituted into Equation 1 to calculate the size of the natural flaw, a_0, that causes failure in unnotched specimens. The variation in a_0 with loading rate is also shown in Fig. 6. It is noted that a_0 values also increase with decreasing rate, and they are on average larger than the expected size of debris and particles within the material of the specimen [12]. Obviously, these cannot be the true size of the inherent flaws pre-existing in the unnotched specimens. They are, however, believed to be the size of crazes at the onset of instability. Therefore, as the loading rate is increased, the amount of the slow crack growth prior to catastrophic failure is decreased until a situation is reached at very high rates when catastrophic brittle failure occurs without any prior stable

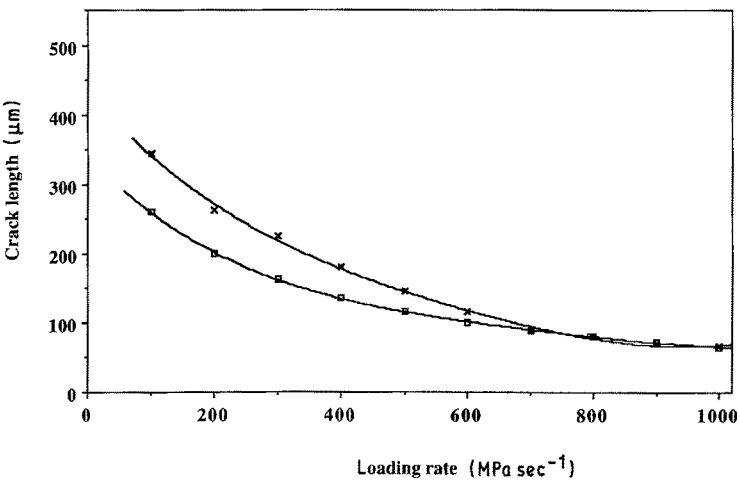

Figure 6 Variations of the minimum flaw size with the loading rate for brittle fracture. (□) a_0, (×) a_m.

crack growth. Therefore the change in the value of a_0 observed in Fig. 6 is suggested to be mainly due to changes in the extent of slow crack growth prior to catastrophic failure rather than the natural flaw size, and a_0 (particularly at lower loading rates) represents the length of the crack after the slow growth region at the onset of instability.

Comparison of the two curves in Fig. 6 shows that for a large section of the loading rate spectrum, (up to $\dot{P} \approx 700\,\text{MPa sec}^{-1}$) the flaw size at instability is lower than the minimum required for brittle fracture. This implies that in this region fracture is not controlled by the size of the flaw. At loading rates above $700\,\text{MPa sec}^{-1}$ the two lines nearly fall on each other and failure seems to be controlled by the flaw length (LEFM). It may, therefore, be concluded that the fracture parameters K_c and G_c measured by testing artificially cracked specimens may be applied to characterized failure of unnotched tubes provided that the loading rate is above $700\,\text{MPa sec}^{-1}$.

The above discussion also explains the difference between the two types of behaviour observed in the fracture stress of pre-notched and unnotched specimens at high rates of loading (Fig. 4). It can be seen that because in the case of unnotched specimens, the length of intrinsic flaw at instability decreases with increasing rate, higher stresses are needed to fracture these specimens at high loading rates. On the other hand, at low rates of loading, due to the slow crack growth prior to catastrophic failure, the specimen breaks at lower values of σ_f.

4. Conclusions

1. Concepts of linear elastic fracture mechanics were successfully applied to characterize the fracture behaviour of thin unplasticized poly(vinyl chloride) tubes at high loading rates.

2. The extent of plastic zone at the tip of the crack was found to decrease continuously with increasing rate. This resulted in a change in the stress state at the tip of the crack, from plane stress to plane strain. The size requirement for valid fracture toughness values was therefore reduced. Values of the crack tip plasticity calculated by Dugdale model were found to "overcorrect" the data, while a more realistic estimate was obtained using the Irwin analysis.

3. While the fracture of pre-notched specimens was found to occur in a completely brittle mode over the whole range of the applied loading rate, in the case of the unnotched specimens, a transition from semi-brittle to brittle mode of failure occurred at about the same loading rate that predominant plane strain situation prevailed.

4. The fracture toughness values measured by testing on artificially cracked specimens may only be used to characterize failure of unnotched tubes at high loading rates (approximately above $700\,\text{MPa sec}^{-1}$). At lower rates the size of inhomogeneities in the material are too small for brittle failure to occur and the yield stress is reached before the fracture stress.

References

1. M. B. JAMARANI, P. E. REED and W. R. DAVIES, *J. Mater. Sci.* **23** (1988) 4437.
2. P. E. REED, P. J. NURSE and E. H. ANDREWS, *ibid.* **9** (1977) (1974).
3. M. B. JAMARANI, PhD thesis, University of London (1986).
4. A. A. GRIFFITH, *Phil. Trans. Roy. Soc. London* **A221** (1920) 163.
5. G. R. IRWIN, *J. Appl. Mech.* **24** (1957) 361.
6. J. EYRING, *J. Chem. Phys.* **4** (1936) 283.
7. C. BAUWENS-CROWET, J. C. BAUWENS and G. HOMES, *J. Polym. Sci. A-2* **7** (1969) 735.
8. H. M. WESTERGAARD, *J. Appl. Mech.* **A49** (1939).
9. A. Y. DARWISH, J. F. MANDELL and F. J. McGARRY, *Polym. Engng Sci.* **22** (1982) 826.
10. M. PARVIN and J. G. WILLIAMS, *Int. J. Fract.* **11** (1975) 963.
11. J. P. BERRY, *J. Appl. Phys.* **34** (1963) 62.
12. S. HASHEMI and J. G. WILLIAMS, *J. Mater. Sci.* **20** (1985) 4202.

Received 9 August
and accepted 21 October 1988